Anal. Chem. **2009,** *81,* 8809–8817

Development of a Linear Ion Trap/Orthogonal-Time-of-Flight Mass Spectrometer for Time-Dependent Observation of Product Ions by Ultraviolet Photodissociation of Peptide Ions

Tae-Young Kim,[†] Jae C. Schwartz,[‡] and James P. Reilly*,[†]

Department of Chemistry, Indiana University, Bloomington, Indiana 47405, and Thermo Electron, 355 River Oaks Parkway, San Jose, California 95134

A hybrid linear ion trap/orthogonal time-of-flight (TOF) mass spectrometer has been developed to observe time-dependent vacuum ultraviolet photodissociation product ions. In this apparatus, a reflectron TOF mass analyzer is orthogonally interfaced to an LTQ using rf-only octopole and dc quadrupole ion guides. Precursor ions are generated by electrospray ionization and isolated in the ion trap. Subsequently they are directed to the TOF source where photodissociation occurs and product ions are extracted for mass analysis. To detect photodissociation product ions having axially divergent trajectories, a large rectangular detector is utilized. With variation of the time between photodissociation and orthogonal extraction in the TOF source, product ions formed over a range of times after photoexcitation can be sampled. Time-dependent observation of product ions following 157 nm photodissociation of a singly charged tryptic peptide ion (NWDAGFGR) showed that prompt photofragment ions (x- and v-type ions) dominate the tandem mass spectrum up to 1 μs after the laser shot, but the intensities of low energy thermal fragment ions (y-type ions) become comparable several microseconds later. Different proton mobilization time scales were observed for arginine- and lysine-terminated tryptic peptides.

Since the invention of electrospray ionization (ESI)[1] and matrix-assisted laser desorption/ionization (MALDI),[2,3] tandem mass spectrometry (MS)[4] has become a pivotal means to obtain sequence and structural information on biomolecules. The most widely used excitation method to generate product ions in tandem MS is collision-induced dissociation (CID),[5−7] typically implemented in triple quadrupole and ion trap mass spectrometers. Low-energy CID that occurs in these instruments involves slow thermal excitation of precursor ions. Activation energy is distributed, and product ions are formed from cleavages of weak bonds, particularly those in the proximity of a mobile proton. The resulting CID tandem mass spectra mainly consist of b- and y-type ions.[8,9] Modifications such as phosphorylations are often lost during low-energy CID processes.[10−12] An alternative method to activate precursor ions in tandem MS is photodissociation.[13,14] It deposits a well-defined energy into precursor ions, is compatible with all types of mass spectrometers, and can localize the activation site when a particular wavelength matches a molecular chromophore. In infrared (IR) photodissociation, multiple photons of light are required to induce bond-cleavage because the energy of a single IR photon is low. This stepwise heating by IR light is analogous to vibrational excitation by multiple collisions in low-energy CID.[15] Thus, tandem mass spectra generated by these two fragmentation methods are generally similar. However, ultraviolet (UV) photodissociation can generate a different fragmentation pattern because it involves electronic excitation.[16]

As the peptide backbone amide has a strong absorption band at around 190 nm,[17] 193 nm ArF excimer laser light (6.4 eV) has been widely employed to photodissociate peptide ions in four-sector,[18] ion cyclotron resonance,[19−22] and tandem time-of-flight

* To whom correspondence should be addressed. E-mail: reilly@indiana.edu.
† Indiana University.
‡ Thermo Electron.

(1) Fenn, J. B.; Mann, M.; Meng, C. K.; Wong, S. F.; Whitehouse, C. M. *Science* **1989**, *246*, 64–71.
(2) Tanaka, K.; Waki, H.; Ido, Y.; Akita, S.; Yoshida, Y.; Yoshida, T. *Rapid Commun. Mass Spectrom.* **1988**, *2*, 151–153.
(3) Karas, M.; Hillenkamp, F. *Anal. Chem.* **1988**, *60*, 2299–2301.
(4) Hernandez, P.; Muller, M.; Appel, R. D. *Mass Spectrom. Rev.* **2006**, *25*, 235–254.
(5) Shukla, A. K.; Futrell, J. H. *J. Mass Spectrom.* **2000**, *35*, 1069–1090.
(6) Wells, J. M.; McLuckey, S. A. *Methods Enzymol.* **2005**, *402*, 148–185.
(7) Laskin, J.; Futrell, J. H. *Mass Spectrom. Rev.* **2003**, *22*, 158–181.
(8) Roepstorff, P.; Fohlman, J. *Biomed. Mass Spectrom.* **1984**, *11*, 601.
(9) Biemann, K. *Biomed. Environ. Mass Spectrom.* **1988**, *16*, 99–111.
(10) Huddleston, M. J.; Annan, R. S.; Bean, M. F.; Carr, S. A. *J. Am. Soc. Mass Spectrom.* **1993**, *4*, 710–717.
(11) Hunter, A. P.; Games, D. E. *Rapid Commun. Mass Spectrom.* **1994**, *8*, 559–570.
(12) Tholey, A.; Reed, J.; Lehmann, W. D. *J. Mass Spectrom.* **1999**, *34*, 117–123.
(13) Dunbar, R. C. *Int. J. Mass Spectrom.* **2000**, *200*, 571–589.
(14) Dunbar, R. C. In *Principles of Mass Spectrometry Applied to Biomolecules*; Laskin, J., Lifshitz, C., Eds.; John Wiley & Sons, Inc.: Hoboken, NJ, 2006; pp 337−377.
(15) Little, D. P.; Speir, J. P.; Senko, M. W.; O'Connor, P. B.; McLafferty, F. W. *Anal. Chem.* **1994**, *66*, 2809–2815.
(16) Bowers, W. D.; Delbert, S. S.; Hunter, R. L.; McIver, R. T. *J. Am. Chem. Soc.* **1984**, *106*, 7288–7289.
(17) Robin, M. B. *Higher Excited States of Polyatomic Molecules*; Academic Press: New York, 1975.
(18) Martin, S. A.; Hill, J. A.; Kittrell, C.; Biemann, K. *J. Am. Soc. Mass Spectrom.* **1990**, *1*, 107–109.
(19) Bowers, W. D.; Delbert, S. S.; McIver, R. T. *Anal. Chem.* **1986**, *58*, 969–972.
(20) Hunt, D. F.; Shabanowitz, J.; Yates, J. R. *J. Chem. Soc. Chem. Commun.* **1987**, 548–550.

10.1021/ac9013258 CCC: $40.75
Published on Web 10/05/2009

(TOF)[23−26] mass spectrometers. Fourth harmonic Nd:YAG laser light at 266 nm (4.7 eV) has been utilized to excite peptide/protein ions containing intact aromatic side chains[27−29] or derivatized with chromophores that absorb at this wavelength.[30−32] Brodbelt and co-workers have applied 355 nm laser light (3.5 eV) to analyze chromophore-derivatized peptides,[33] oligosaccharides,[34] and crown-ether complexes,[35] and the Dugourd group has explored various UV wavelengths (220−280 nm) to study peptide ions with multistage MS.[36−38] We have exploited vacuum UV light at 157 nm (7.9 eV) to photodissociate singly charged peptide ions in a home-built MALDI tandem TOF instrument[39] and extended its applications to the analyses of peptide/protein ions,[40−42] oligosaccharides,[43,44] and lipids[45] in a linear ion trap mass spectrometer. Zubarev and co-workers also showed that 157 nm photodissociation induces a facile cleavage of disulfide bonds in peptide/protein polycations[46] and can probe gas-phase zwitterionic states of peptides.[47]

An ion trap mass spectrometer with an ESI source has some advantages for studying ion photodissociation compared with a MALDI tandem TOF instrument, though the latter has been a popular platform for this type of experiment. ESI generates multiple charge state ions whose internal energy is relatively low and well-defined. An ion trap instrument provides good precursor ion mass selection, noncritical timing of photodissociation events, and multistage MS performance that can involve various combinations of photodissociation and CID. However, relative to tandem-TOF instruments, the analysis time following photodissociation in the ion trap is slow, on the order of milliseconds. In this study, an ESI linear ion trap/orthogonal-TOF (LIT/o-TOF) mass spectrometer was built to achieve a faster analysis time following photodissociation of peptide ions by vacuum UV light. A few groups have previously reported on experiments related to this instrument. Douglas and co-workers have demonstrated CID tandem MS capabilities of ESI LIT/o-TOF mass spectrometers.[48,49] Gabryelski and Li have developed an ion trap/TOF instrument for photodissociation studies.[27] They recorded 266 nm photodissociation mass spectra of protonated di- and tripeptides as a function of the time delay between photoexcitation inside the trap and extraction for TOF detection from 1.5 μs to several milliseconds. In their experiments, photodissociation occurred inside the ion trap. In the present work it takes place in the TOF source region, enabling us to extract fragment ions formed at short times after photodissociation. This experiment necessitated the transfer of precursor ions from the ion trap, which led to some complications associated with product ions following axially divergent trajectories to the detector. Our approaches to reducing the size of the ion beam in the TOF source and for optimizing the sensitivity of the instrument are discussed. Time-resolved spectra of product ions generated by 157 nm photodissociation of a singly charged tryptic peptide are presented, and some of the unique characteristics of these spectra discussed. The time-dependent mobilization of protons is also directly observed in 157 nm photodissociation tandem mass spectra of singly charged peptides FSWGAEGQ**R** and FSWGAEGQ**K**.

EXPERIMENTAL SECTION

Materials. Angiotensin II, FSWGAEGQR, and caffeine were purchased from Sigma (St. Louis, MO). FSWGAEGQK and NWDAGFGR were synthesized at Sigma-Genosys (Woodlands, TX). Methanol (MeOH) and glacial acetic acid were supplied from Fisher (Fair Lawn, NJ) and Mallinckrodt Baker (Philipsburg, NJ), respectively. Peptide stock solutions were prepared in water/MeOH (1:1, v/v) and diluted to 5−10 μM using 1% acetic acid in MeOH.

Apparatus. A schematic diagram of the LIT/o-TOF mass spectrometer with an ESI source is shown in Figure 1. The instrument was set up by orthogonal coupling of a reflectron TOF mass analyzer to an LTQ ion trap (Thermo Electron, San Jose, CA) with an ion guide consisting of an rf-only octopole and a dc quadrupole, after simulating ion trajectories with Simion 8.0 (Scientific Instrument Services, Ringoes, NJ).

Detection of fragment ions formed in the TOF source requires an arrangement of the reflector and detector that is different from a conventional o-TOF mass analyzer. In a normal quadrupole/o-TOF tandem mass spectrometer employing CID for fragmentation of precursor ions, different product ions are generated in the collision cell. Since they are accelerated toward the TOF source region with the same energy, smaller ions have higher axial

(21) Williams, E. R.; Furlong, J. J. P.; McLafferty, F. W. *J. Am. Soc. Mass Spectrom.* **1990**, *1*, 288–294.
(22) Guan, Z. Q.; Kelleher, N. L.; O'Connor, P. B.; Aaserud, D. J.; Little, D. P.; McLafferty, F. W. *Int. J. Mass Spectrom.* **1996**, *158*, 357–364.
(23) Barbacci, D. C.; Russell, D. H. *J. Am. Soc. Mass Spectrom.* **1999**, *10*, 1038–1040.
(24) Morgan, J. W.; Hettick, J. M.; Russell, D. H. *Methods Enzymol.* **2005**, *402*, 186–209.
(25) Moon, J. H.; Yoon, S. H.; Kim, M. S. *Rapid Commun. Mass Spectrom.* **2005**, *19*, 3248–3252.
(26) Moon, J. H.; Shin, Y. S.; Cha, H. J.; Kim, M. S. *Rapid Commun. Mass Spectrom.* **2007**, *21*, 359–368.
(27) Gabryelski, W.; Li, L. *Rev. Sci. Instrum.* **1999**, *70*, 4192–4199.
(28) Oh, J. Y.; Moon, J. H.; Kim, M. S. *Rapid Commun. Mass Spectrom.* **2004**, *18*, 2706–2712.
(29) Oh, J. Y.; Moon, J. H.; Kim, M. S. *J. Mass Spectrom.* **2005**, *40*, 899–907.
(30) Oh, J. Y.; Moon, J. H.; Lee, Y. H.; Hyung, S. W.; Lee, S. W.; Kim, M. S. *Rapid Commun. Mass Spectrom.* **2005**, *19*, 1283–1288.
(31) Diedrich, J. K.; Julian, R. R. *J. Am. Chem. Soc.* **2008**, *130*, 12212–12213.
(32) Ly, T.; Julian, R. R. *J. Am. Chem. Soc.* **2008**, *130*, 351–358.
(33) Wilson, J. J.; Brodbelt, J. S. *Anal. Chem.* **2007**, *79*, 7883–7892.
(34) Wilson, J. J.; Brodbelt, J. S. *Anal. Chem.* **2008**, *80*, 5186–5196.
(35) Wilson, J. J.; Kirkovits, G. J.; Sessler, J. L.; Brodbelt, J. S. *J. Am. Soc. Mass Spectrom.* **2008**, *19*, 257–260.
(36) Tabarin, T.; Antoine, R.; Broyer, M.; Dugourd, P. *Rapid Commun. Mass Spectrom.* **2005**, *19*, 2883–2892.
(37) Lemoine, J.; Tabarin, T.; Antoine, R.; Broyer, M.; Dugourd, P. *Rapid Commun. Mass Spectrom.* **2006**, *20*, 507–511.
(38) Joly, L.; Antoine, R.; Broyer, M.; Dugourd, P.; Lemoine, J. *J. Mass Spectrom.* **2007**, *42*, 818–824.
(39) Thompson, M. S.; Cui, W.; Reilly, J. P. *Angew. Chem., Int. Ed.* **2004**, *43*, 4791–4794.
(40) Kim, T.-Y.; Thompson, M. S.; Reilly, J. P. *Rapid Commun. Mass Spectrom.* **2005**, *19*, 1657–1665.
(41) Zhang, L. Y.; Cui, W.; Thompson, M. S.; Reilly, J. P. *J. Am. Soc. Mass Spectrom.* **2006**, *17*, 1315–1321.
(42) Zhang, L.; Reilly, J. P. *J. Am. Soc. Mass Spectrom.* **2008**, *19*, 695–702.
(43) Devakumar, A.; Mechref, Y.; Kang, P.; Novotny, M. V.; Reilly, J. P. *Rapid Commun. Mass Spectrom.* **2007**, *21*, 1452–1460.
(44) Devakumar, A.; Mechref, Y.; Kang, P.; Novotny, M. V.; Reilly, J. P. *J. Am. Soc. Mass Spectrom.* **2008**, *19*, 1027–1040.
(45) Devakumar, A.; O'Dell, D. K.; Walker, J. M.; Reilly, J. P. *J. Am. Soc. Mass Spectrom.* **2008**, *19*, 14–26.
(46) Fung, Y. M. E.; Kjeldsen, F.; Silivra, O. A.; Chan, T. W. D.; Zubarev, R. A. *Angew. Chem., Int. Ed.* **2005**, *44*, 6399–6403.
(47) Kjeldsen, F.; Silivra, O. A.; Zubarev, R. A. *Chem.—Eur. J.* **2006**, *12*, 7920–7928.
(48) Campbell, J. M.; Collings, B. A.; Douglas, D. J. *Rapid Commun. Mass Spectrom.* **1998**, *12*, 1463–1474.
(49) Collings, B. A.; Campbell, J. M.; Mao, D.; Douglas, D. J. *Rapid Commun. Mass Spectrom.* **2001**, *15*, 1777–1795.

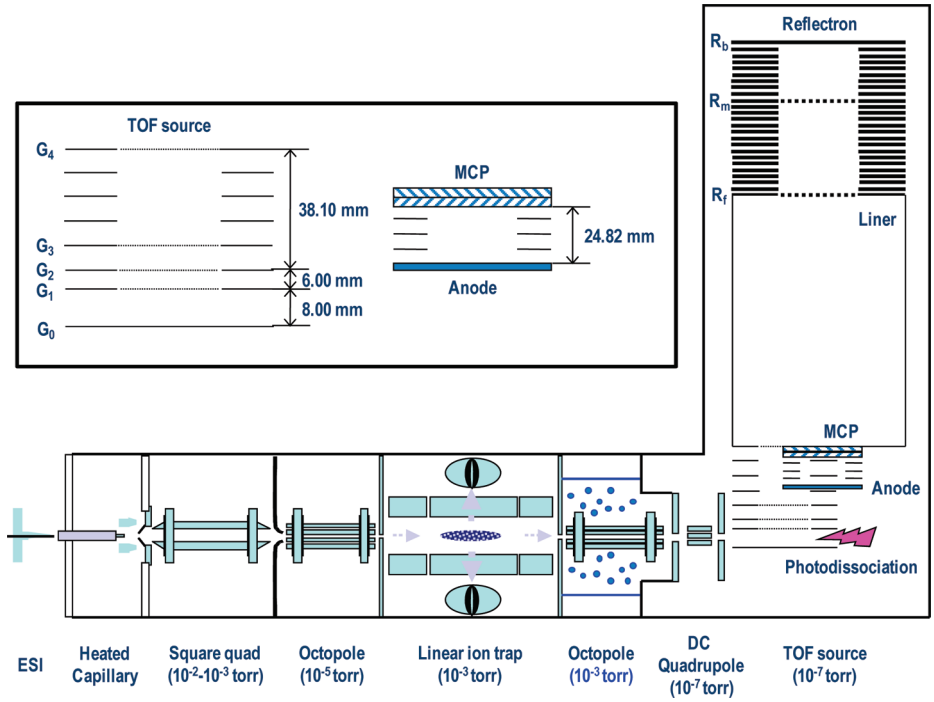

Figure 1. Top view schematic diagram of the ESI LIT/o-TOF mass spectrometer. The reflectron is in the same horizontal plane as the LIT and TOF source, but the detector is located below this plane. The inset shows the dimensions of gaps in the source and detector. The gaps between G_2 and G_4 in the source and between the back microchannel plate (MCP) and anode are evenly divided with the ring electrodes.

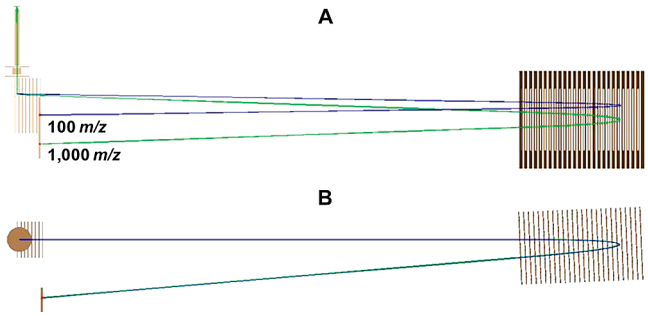

Figure 2. SIMION simulation showing two trajectories of 1 000 *m/z* precursor ions and 100 *m/z* product ions after photodissociation in the TOF source. (A) Top and (B) side views.

velocities and larger ones smaller velocities. Upon orthogonal extraction in the TOF source, lighter ions are given higher orthogonal velocities and heavier ions smaller velocities. Thus the trajectories of heavy and light fragments are parallel to one another and a detector comparable in size to the TOF source is adequate. In our experiments, however, precursor ions of a single mass are isolated in the trap. They reach the TOF source region with practically the same axial velocity because they exit the trap with a well-defined initial kinetic energy. Product ions orthogonally extracted after photodissociation show axially divergent trajectories to the detector, since the axial velocity components are almost all the same while the orthogonal velocity components are still highly mass dependent. Consequently, a large detector (50.8 mm × 101.6 mm) is needed. The axially diverging trajectories of product ions also affect the position of the detector. SIMION simulations comparing trajectories of 1 000 m/z precursor ions and 100 m/z photofragment ions are displayed in a view from above in Figure 2A. The axial displacements of the 100 m/z product ions are smaller than those of the precursor ions. Because of the large differences between the axial and orthogonal velocity components of product ions, the axial displacements of products ions are smaller than the size of the ion source preventing the detector from being placed beside the TOF source as in a normal o-TOF mass spectrometer. For this reason, the detector is located below the TOF source and the ion reflector is tilted downward toward the detector as shown in the Figure 2B side view.

Axial Ejection of Ions from LTQ. In the normal operation of the LTQ ion trap, ions are radially scanned out toward two electron multiplier tubes located on both sides of the trap. Axial ion ejection was enabled by replacing several procedure files with modified ones. For axial ion ejection, ions are first moved into the back section of the trap and then ejected by an extraction pulse applied to the back lens after a period of collisional damping. The method of axial ejection used here is similar to that utilized in the Fourier transform ion cyclotron resonance (FTICR) and orbitrap hybrid versions of the instrument; however, the exact voltages and timing have been somewhat modified for this application. Details about how this is accomplished are discussed in the Supporting Information.

Mass Spectrometry. All samples were infused into the LTQ mass spectrometer with a homemade nanospray source of 75 μm i.d. fused-silica capillary (Polymicro Technologies, Phoenix, AZ) pulled into a tip needle. The tip was held at 1.8 kV, and the liquid flow rate was 200 nL/min. The maximum ion injection time was set to 700 ms with the automatic gain control (AGC) on. The AGC target value for MS^n was set to $3-5 \times 10^4$ in order to increase the number of singly charged ions for photodissociation. An isolation width of 0.7 m/z was chosen to select precursor ions. This efficiently removed the contribution from ^{13}C to mass spectral peaks. To monitor the profile of ions arriving at the TOF source, the TOF source was removed and replaced by

an electron multiplier tube (EMT) detector (4715, Burle Industries, Lancaster, PA). For the detection of ions, −15 and −1.5 kV were applied to the conversion dynode and the entrance end of the EMT, respectively. No grid electrode was used to define the electric field in the TOF source between the ion collimating lens and the EMT. This shifts the absolute arrival times of ions a little shorter but does not distort the arrival patterns of ions at the TOF source region. Ion current from the EMT was directed to a 1 GS/s oscilloscope (LeCroy 9370, LeCroy Corp., Chestnut Ridge, NY) and a hundred pulses of ejected ions were averaged to obtain the distribution of ion arrival times at the EMT detector.

An F_2 laser (EX100HF-60, GAM Laser, Orlando, FL) was connected to the TOF source chamber with a vacuum line. A single, unfocused 10 ns, 2 mJ F_2 laser pulse having a 5 mm × 10 mm cross section was used for photodissociation. Photodissociation experiments can be performed either inside the LIT or in the TOF source, since the F_2 laser was aligned coaxially with the LIT and through the TOF source. However, only tandem mass spectra obtained from photodissociation in the TOF source are presented here. For photodissociation in the TOF source, precursor ions isolated in the ion trap were transferred into the TOF source region by the axial ion ejection process described in the preceding section. The negative-going edge of the ion ejection pulse on the back lens of the LTQ was used to trigger a BNC delay generator (555, San Rafael, CA) that controls all timing for the laser, digitizer, and push/pull pulses. The signal collected on the reflectron detector anode was sent to a home-built high-speed amplifier. The amplified signal was digitized by an Acqiris digitizer (DP210, Agilent Technologies, Santa Clara, CA) with 500 MHz bandwidth and a 2 GHz sampling rate. An acquisition program previously developed for photodissociation experiments in a MALDI tandem TOF analyzer[50] was employed to average data from multiple laser shots. The program has a function to separately sum and save spectra collected from alternate shots. In one application, the photodissociation laser is triggered on alternate axial ion ejection pulses in order to calculate the extent of precursor ion depletion. Comparison of precursor ion peak intensities measured with and without photodissociation indicated that 25−40% of the ions were fragmented. In a second application, the photodissociation laser is triggered in and out of synchronization with ions ejected from the trap. Subtraction of the two spectra leads to information about the production of photoions. This resulted in photodissociation tandem mass spectra containing very few photoions, which are mainly distributed at masses below 300 m/z. A total of 4 000 laser shots were summed to acquire a photodissociation tandem mass spectrum. High-frequency noise was filtered by 10 point-FFT smoothing in OriginPro 7.0 (OriginLab, Northampton, MA) before calibration. Mass calibration of a photodissociation spectrum is performed using a home-built software.[51] Masses of the precursor, immonium, and product ions are utilized as mass calibrants.

(50) Thompson, M. S. Doctoral Thesis, Indiana University, Bloomington, IN, 2007.

(51) Christian, N. P. Doctoral Thesis, Indiana University, Bloomington, IN, 2000.

RESULTS AND DISCUSSION

Arrival of Ions in the TOF Source. In order to obtain photodissociation TOF mass spectra with a high sensitivity, it is important to minimize ion beam spreading and loss of ions during the transfer process between the ion trap and the TOF source. The two key parameters to reduce the axial ion beam spreading were the fall time of the extraction pulse applied to the back lens and the collisional damping time that ions spend in the back section of the trap before exiting. A 40 V extraction pulse generated internally by the LTQ had a 90 μs fall time. To test the effect of the fall time on the transport of extracted ions to the TOF source, a circuit was constructed to produce a rapidly falling voltage pulse (a few μs for 40 V). An electron multiplier was mounted in the TOF source region in order to monitor the arrival of ions from the ion trap under various axial extraction conditions. Figure 3 displays the time-dependent detector output for caffeine (m/z 195) ions extracted using the original LTQ pulse and with the faster pulse for different collisional damping times before axial ion ejection from the back section of the trap. Note that in each case a sharp peak was followed by a broad one. The sharp peaks appear to originate from ions located between the back section and back lens of the trap. These ions are immediately extracted to the TOF source by the axial extraction pulse. The broad peaks apparently result from ions within the back section. The axial electric field generated between the back section and back lens penetrates somewhat into the back section of the trap. Upon application of the axial extraction pulse, ions having different initial axial velocities and positions within the back section of the trap are extracted over a range of times resulting in broad arrival peaks. Similar profiles were observed in SIMION simulations of ions extracted from an octopole ion trap by Marshall and co-workers.[52] As the collisional damping time increased from 3 to 8 ms, the peak width in the TOF source region decreased and the peak location moved to longer times (Figure 3A). Further increase in the damping time from 8 to 15 ms resulted in only a slight decrease in the peak width, and there was no perceptible change when the time was extended from 15 to 30 ms. Ions gain kinetic energy corresponding to the dc offset voltage difference between the center and back sections when they move into the back section of the trap. Ions gradually lose this energy by collisions with buffer gas while residing in the back section. Insufficient collisional damping times widen the TOF source arrival profile. Compared with the original LTQ pulse, the use of an extraction pulse with a faster fall time resulted in narrower ion peak widths and increased peak intensities as seen in Figure 3B. Since the slow fall time of the original LTQ pulse generates a time-dependent axial electric potential gradient between the back section and back lens, ions exiting the ion trap immediately after applying the extraction pulse gain less kinetic energy than those passing the back lens later. The fast pulse provides all extracted ions with approximately the same axial extraction energy since a full axial electric field is developed before most ions exit through the back lens. On the basis of these observations, 15 ms of collisional damping time and the fast back lens pulse were employed in our TOF photodissociation experiments.

(52) Wilcox, B. E.; Hendrickson, C. L.; Marshall, A. G. *J. Am. Soc. Mass Spectrom.* **2002**, *13*, 1304–1312.

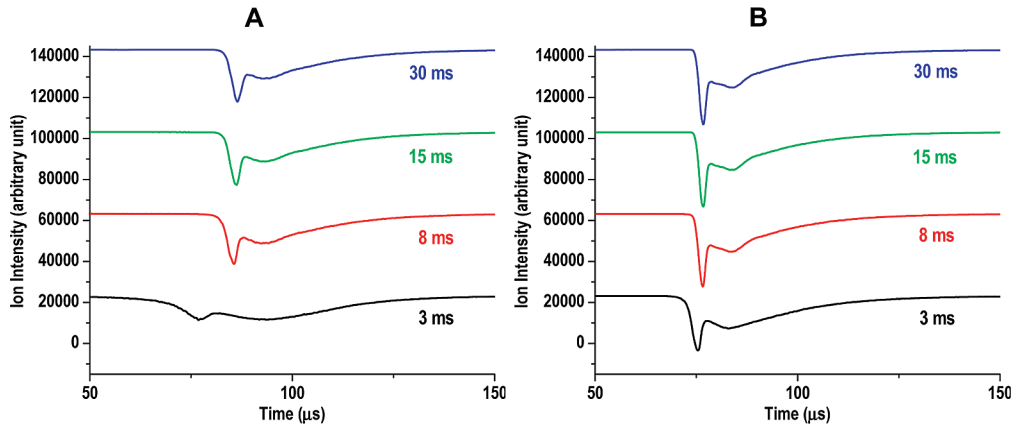

Figure 3. Time-dependent output recorded with the EMT in the TOF source region for caffeine (*m*/*z* 195) using (A) the original LTQ and (B) faster pulses with different collisional damping time in the back section of the trap before exiting.

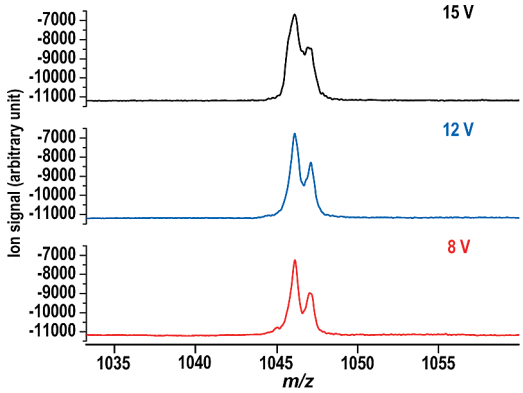

Figure 4. LIT/o-TOF mass spectra of angiotensin II (*m*/*z* = 1046.5) using different axial extraction voltages on the LTQ back lens without a collisional damping chamber.

Factors that Affect the Resolution of an o-TOF Mass Spectrum. Experimental parameters associated with the transfer of ions from the trap to the TOF detector were varied to observe their influence on the resolution of o-TOF mass spectra. Figure 4 displays LIT/o-TOF mass spectra of singly charged angiotensin II using different axial extraction potentials on the LTQ back lens without a collisional damping chamber for the transfer octopole located between the ion trap and the dc quadrupole. Precursor ion selection was set to 1.5 *m*/*z* for this study. When the extraction potential on the LTQ back lens was lowered from 15 to 8 V, the resolution of the instrument increased from 1 250 to 1 720 but the peak intensity slightly decreased. A higher axial extraction voltage can penetrate deeper into the back section in the trap and extract more ions to the TOF source. However, it creates a wider spatial and kinetic energy ion distribution on the TOF axis before orthogonal acceleration and exacerbates space charge effects owing to the larger number of ions. In summary, the application of a higher axial extraction potential increases the sensitivity but decreases the resolution of the LIT/o-TOF instrument.

A collisional damping chamber was implemented into the transfer octopole between the LIT and dc quadrupole to study the effect of damping gas (He) pressure on mass resolution. The pressure of the octopole section without the damping chamber is as low as 8×10^{-6} Torr because it is exposed to the region where the LTQ's electron multipliers are placed. The pressure inside the damping chamber was 3 mTorr without injection of buffer gas. This pressure was elevated as a result of buffer gas entering from the 3 mTorr ion trap into the enclosed octopole section through the aperture on the back lens and the deliberately slow evacuation of this region. The observed dependence of mass resolution on damping pressure in the transfer octopole region is displayed in Figure S2 in the Supporting Information. Mass resolution of the instrument reached 1 960 at 3 mTorr and decreased with increasing damping pressure. Unfortunately, an increase in mass resolution resulted in loss of sensitivity: Because collisional damping makes an ion beam spread out axially, the higher He gas pressure led to lower signal intensity. Higher pressure in the transfer octopole section also required a smaller aperture (from 1.524 to 0.508 mm in diameter) for the differential pumping lens between the dc quadrupole and TOF source in order to maintain high vacuum in the TOF mass spectrometer. Since sensitivity was more important than resolution for our initial experiments, the collisional damping chamber was removed for subsequent peptide photofragmentation studies.

The limited resolution in our LIT/o-TOF mass spectrometer can be attributed to several factors arising from the instrument design. First, the need for a large detector to cover axially divergent product ions resulted in the use of microchannel plates with a large pore size (25 μm). Second, the octopole in the ion guide optics causes a wider spatial distribution of ions along the o-TOF axis compared with a quadrupole. A quadrupole has less charge capacity inside the device but generates more focused ions on-axis than an octopole.[53] Third, the abnormal location of the detector required that the ion reflector be tilted by 3° from the normal, so ions pass through grids nonorthogonally to the grid surface. Ions that do not pass perpendicularly through the center of a grid hole are dispersed according to their positions and incident angles and arrive over a range of times at the detector.[54] While using rectangular mesh grid can alleviate this effect on the longer dimension, which is inherent to an o-TOF mass spectrometer, tilting the ion reflector exacerbates it in the shorter dimension adversely affecting mass resolution. Fourth, the number of ions per each TOF analysis in our instrument is much higher

(53) Tolmachev, A. V.; Udseth, H. R.; Smith, R. D. *Anal. Chem.* **2000**, *72*, 970–978.
(54) Dawson, J. H. J.; Guilhaus, M. *Rapid Commun. Mass Spectrom.* **1989**, *3*, 155–159.

than that in a conventional o-TOF mass spectrometer. In a normal o-TOF mass analyzer, ions are (quasi-)continuously introduced into the TOF source and pulsed into the mass spectrometer at a few kilohertz repetition rate. Thus, only a few are injected into the TOF source in each pulse.[55] In contrast, the number of ions in a pulse brought to the TOF source for mass analysis is several orders of magnitude higher in our experiments. The high charge density in the TOF source may induce a significant space charge effect that widens the spatial distribution of ions on the TOF axis. Although the last two issues are inherent limitations for the photodissociation experiment in the TOF source, the first two problems could be mitigated by using MCPs with a smaller pore size and replacing the octopole with a quadrupole.

Time-Dependent Photodissociation Tandem Mass Spectra. In order to maximize the photodissociation cross-sectional volume, the laser light was coaxially aligned with the LIT. This configuration facilitated the recording of photodissociation mass spectra with different time delays between the laser and orthogonal acceleration pulses. The timing sequence for photodissociation in the TOF source is displayed in Figure S3 in the Supporting Information. Time-dependent tandem mass spectra of singly charged NWDAGFGR obtained by 157 nm photodissociation are shown in Figure 5. The spectrum in Figure 5A was recorded with a time delay of 300 ns. A complete series of x-type ions (from x_1 to x_7) and a few v-type ions (v_3, v_5, and v_7) were generated as major fragments. Production of these types of fragment ions by 157 nm photodissociation was previously reported.[39,40,56,57] Peptide ions having C-terminal basic residues yield x + 1 ions by homolytic radical cleavage between the α- and carbonyl-carbons in the peptide backbone. Loss of hydrogen atoms or side chain radicals from x + 1 ions forms even-electron fragments or x-, v-, and w-type ions. The detection of a strong x + 1 ion (x_7 + 1) supports this photodissociation mechanism. As seen in examples below, high mass x + 1 ions were commonly observed adjacent to x ions following the 157 nm photodissociation of C-terminal basic peptides. This is noteworthy, because in MALDI tandem TOF experiments, a + 1 ions were detected following 157 nm photodissociation of N-terminal arginine peptides but x + 1 ions were not observed with C-terminal arginine peptides.[56] The higher stability of the α-carbon relative to the carbonyl-carbon radical ions[58] explains this discrepancy. Because electrosprayed and collisonally cooled precursor ions have low internal energies, x + 1 ions not previously observed in MALDI TOF−TOF experiments are now detectable for some time after photodissociation. Recently, Berkout has also observed these radical ions in tandem mass spectra of singly charged C-terminal basic peptides obtained via interaction with metastable rare gas atoms in an ESI o-TOF mass spectrometer.[59] He proposed that high-energy excitation of peptide ions by metastable noble gas atoms initiates the homolytic radical cleavage of the α- and carbonyl-carbon bond leading to x + 1 ions. Also evident in Figure 5A is a loss of the side chain of an amino acid (labeled by m_2) along with the tryptophan immonium ion (labeled W). Although some other types of fragments such as y-, Y-, and z-ions also appear, x- and v-type ions are major product ions formed within 300 ns after photoexcitation. The tandem mass spectrum recorded with a 1 μs ion extraction delay (Figure 5B) is quite similar. Minor differences between the two spectra include the appearance of y_2 and w_6 and some growth in y_3, y_6, and z_3. Despite the increased time delay, x- and v-type ions are still dominant peaks 1 μs after photodissociation. When the time delay was increased to 5 μs (Figure 5C), a full series of y-type ions (y_1 to y_7) were observed with peak intensities comparable to those of x-type ions. Some weak features corresponding to internal fragments (I) and NH_3-loss y-type ions (y_1*, y_3*, and y_7*) also appear. More significantly, some N-terminal fragment ions (a_2, b_2, b_3, and b_7) also appear with this time delay indicating that the charge proton is no longer sequestered on the arginine at this time. After 13 μs (Figure 5D), peak intensities of y-type and N-terminal ions further increased and two additional ions (b_5 and a_6) appear in the spectrum.

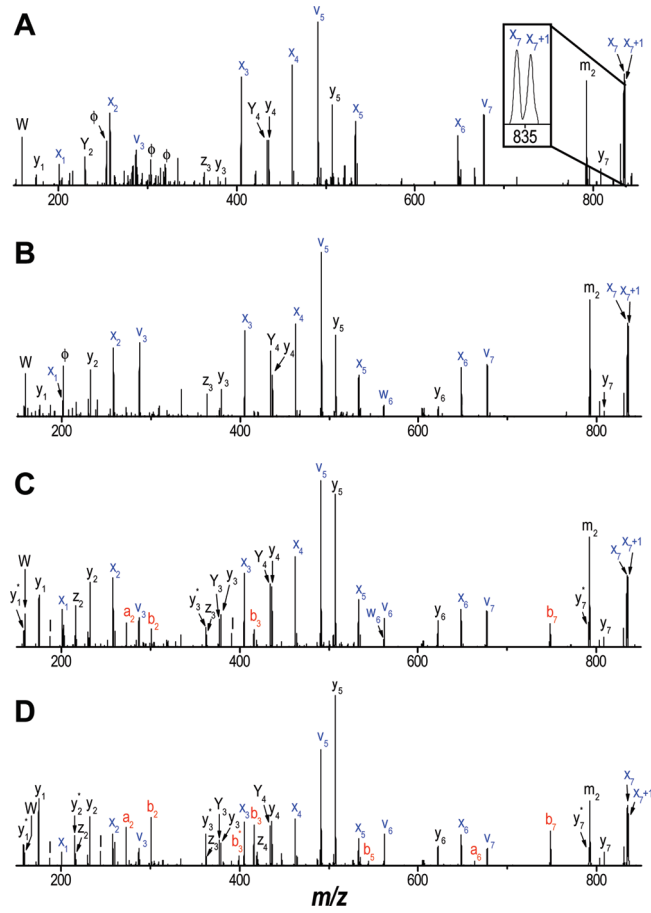

Figure 5. Tandem mass spectra by 157 nm photodissociation of NWDAGFGR with time delays between photoexcitation and mass analysis of (A) 300 ns, (B) 1 μs, (C) 5 μs, and (D) 13 μs. Ions arising from loss of NH_3 are labeled with superscripts of * and loss of amino acid side chains from $[M + H]^+$ is denoted as m. Internal fragment ions and photoions are labeled with I and ϕ, respectively, and W represents an immonium ion of tryptophan. The inset shows the presence of x + 1 radical ions.

(55) Krutchinsky, A. N.; Loboda, A. V.; Spicer, V. L.; Dworschak, R.; Ens, W.; Standing, K. G. *Rapid Commun. Mass Spectrom.* **1998**, *12*, 508–518.
(56) Cui, W.; Thompson, M. S.; Reilly, J. P. *J. Am. Soc. Mass Spectrom.* **2005**, *16*, 1384–1398.
(57) Reilly, J. P. *Mass Spectrom. Rev.* **2009**, *28*, 425–447.
(58) O'Connor, P. B.; Lin, C.; Cournoyer, J. J.; Pittman, J. L.; Belyayev, M.; Budnik, B. A. *J. Am. Soc. Mass Spectrom.* **2006**, *17*, 576–585.
(59) Berkout, V. D. *Anal. Chem.* **2009**, *81*, 725–731.

In summary, 157 nm photodissociation of singly charged NWDAGFGR resulted in tandem mass spectra dominated by high-energy photofragment ions (x- and v-type ions) up to 1 μs after photoexcitation. At longer time delays, peak intensities of product ions generated by thermal (ergodic) fragmentation processes (y-type and N-terminal fragment ions) increased. After 5 μs they became comparable to signals of prompt photofragment ions. Thermal fragmentation can occur through two pathways after photoexcitation. First, the primary photofragment x-, v-, and w-type ions may undergo secondary thermal fragmentation processes using internal excitation derived from the photodissociation process. Second, a chromophore other than the peptide backbone amide groups absorbs the light. In this case, the electronic excitation, instead of rapidly inducing α- and carbonyl-carbon bond dissociation, is converted into vibrational energy that is rapidly randomized and induces thermal fragmentation. N-terminal fragment ions are presumably generated by the second pathway since x-type ions cannot produce them. These two pathways can be distinguished from each other by investigating time-dependent changes in absolute peak intensities of precursor and product ions. With an increased time delay, the first mechanism would predict decreasing x-type ion signals, while from the second mechanism one would anticipate decreasing precursor ion signals. Unfortunately, the current experimental conditions do not provide consistent precursor ion yields so this could not be tested. As described in the Experimental Section, a total of 4 000 laser shots with a repetition rate of 2−3 Hz were used to generate a photodissociation tandem mass spectrum. A long data acquisition time (25−35 min) results in significantly varying absolute peak intensities of precursor ions from one spectrum to another, which also affects absolute peak intensities of all product ions. Despite this, relative peak intensities among different types of product ions were quite consistent in tandem mass spectra with the same time delay. Therefore, relative peak intensities of product ions in the time-dependent photodissociation experiments can be legitimately compared and all tandem mass spectra are normalized to the base peaks.

Mobile Proton Effects on Time-Dependent Photodissociation Tandem Mass Spectra. The "mobile proton model" is popularly employed to understand peptide fragmentation in the gas phase.[60−63] It is generally accepted that a charged proton that initiates peptide backbone cleavages to generate b-/y-type ions is easily mobilized if there are more protons than arginines in the sequence.[64−66] In order to examine the effect of mobile protons on time-dependent photodissociation tandem mass spectra, 157 nm photodissociation of two singly charged peptides having the same sequence except for their C-terminal basic residues

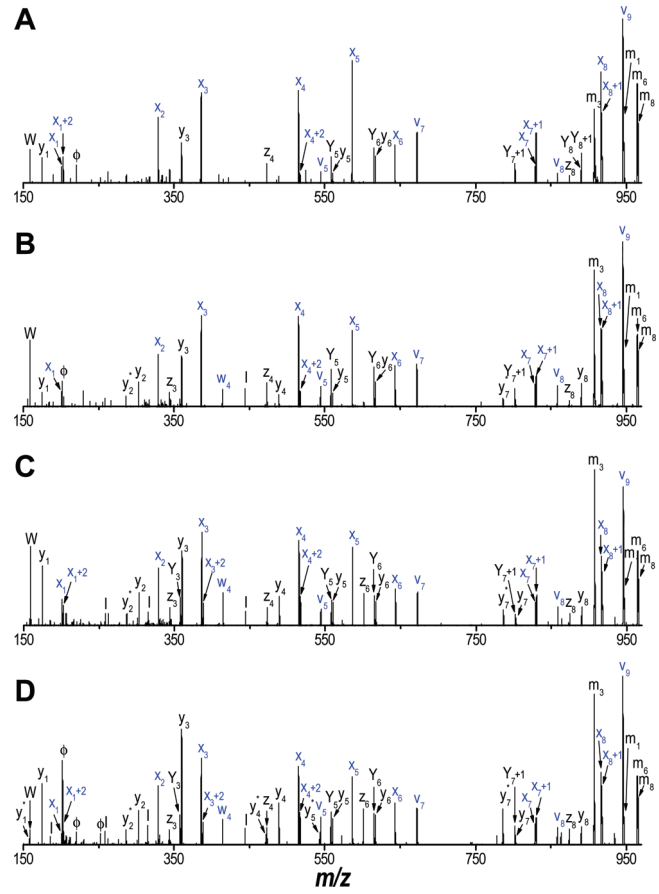

Figure 6. Tandem mass spectra by 157 nm photodissociation of FSWGAEGQ**R** with time delays between photoexcitation and mass analysis of (A) 300 ns, (B) 1 μs, (C) 5 μs, and (D) 13 μs.

(FSWGAEGQ**R** and FSWGAEGQ**K**) was performed with different time delays between laser irradiation and mass analysis. Figure 6 displays data for singly charged FSWGAEGQ**R**. The tandem mass spectrum recorded with a time delay of 300 ns (Figure 6A) shows a complete series of x-type ions (from x_1 to x_8) as major product ions along with some v-type ions (v_5, v_7, v_8, and v_9). Two x + 1 ions (x_7 + 1 and x_8 + 1) that are consistent with our photodissociation mechanism appear in the high mass region. Losses of the side chain of some amino acids from the precursor ions (labeled with m_1, m_3, m_6, and m_8), a tryptophan immonium ion, and some y-, Y-, and z-ions are also observed. Figure 6A is qualitatively comparable to Figure 5A in that high-energy photofragment ions (x- and v-type ions) are the main product ions. A minor difference between the two mass spectra is that some low *m/z* x-ions are accompanied by the corresponding x + 2 ions (x_1 + 2 and x_4 + 2) in Figure 6A. These unusual ions seem to be generated by a transfer or rearrangement of a hydrogen atom onto x + 1 ions. A similar 1 Da mass increase has been reported for radical z-ions in ECD.[67] The tandem mass spectrum obtained with a time delay of 1 μs (Figure 6B) shows a small increase in the number of product ions. Appearance of y-type ions with NH_3 loss (y_2* and y_7*), one internal fragment (I), and additional y-type ions (y_2 and y_4) can be attributed to thermal fragmentation processes after photoexcitation. Despite the

(60) Burlet, O.; Orkiszewski, R. S.; Ballard, K. D.; Gaskell, S. J. *Rapid Commun. Mass Spectrom.* **1992**, *6*, 658–662.
(61) Cox, K. A.; Gaskell, S. J.; Morris, M.; Whiting, A. *J. Am. Soc. Mass Spectrom.* **1996**, *7*, 522–531.
(62) Dongre, A. R.; Jones, J. L.; Somogyi, A.; Wysocki, V. H. *J. Am. Chem. Soc.* **1996**, *118*, 8365–8374.
(63) Wysocki, V. H.; Tsaprailis, G.; Smith, L. L.; Breci, L. A. *J. Mass Spectrom.* **2000**, *35*, 1399–1406.
(64) Tsaprailis, G.; Nair, H.; Somogyi, A.; Wysocki, V. H.; Zhong, W. Q.; Futrell, J. H.; Summerfield, S. G.; Gaskell, S. J. *J. Am. Chem. Soc.* **1999**, *121*, 5142–5154.
(65) Gu, C. G.; Somogyi, A.; Wysocki, V. H.; Medzihradszky, K. F. *Anal. Chim. Acta* **1999**, *397*, 247–256.
(66) Tsaprailis, G.; Somogyi, A.; Nikolaev, E. N.; Wysocki, V. H. *Int. J. Mass Spectrom.* **2000**, *196*, 467–479.
(67) Zubarev, R. A.; Horn, D. M.; Fridriksson, E. K.; Kelleher, N. L.; Kruger, N. A.; Lewis, M. A.; Carpenter, B. K.; McLafferty, F. W. *Anal. Chem.* **2000**, *72*, 563–573.

slightly increased spectral complexity, x- and v-type ions are still dominant peaks 1 μs after photoexcitation. The tandem spectrum obtained with a time delay of 5 μs (Figure 6C) displays somewhat increased peak intensities of y- and y*-type ions relative to x- and v-type ions. This trend seems to continue at a time delay of 13 μs (Figure 6D). In this case, the intensities of high-energy x- and v-type and thermal y-type ions are roughly comparable.

It is noteworthy that no N-terminal fragment ions are observed for FSWGAEGQ**R** up to 13 μs after photoexcitation. This is strikingly different from the photodissociation mass spectra of NWDAGFGR where N-terminal product ions appeared with a time delay of 5 μs or longer. The side chain of arginine is obviously the most favorable site for the charge proton because of its high gas-phase basicity.[68] Thus, generation of N-terminal fragment ions from C-terminal arginine-containing peptides necessitates the proton movement from the arginine side chain to the N-terminal side. Since both peptides (FSWGAEGQ**R** and NWDAGFG**R**) contain arginine at the C-terminus, the gas phase basicity of arginine cannot be the sole factor that determines whether a charge can be mobilized. Perhaps a structural difference between the two peptides facilitates the proton transfer that leads to N-terminal fragment ions from NWDAGFGR.

Lysine is considerably less basic than arginine.[68] To investigate the effect that this has on the mobilization of charge, time-dependent 157 nm photodissociation of singly charged peptide FSWGAEGQ**K** was performed. Figure 7A displays the tandem mass spectrum recorded with a time delay of 300 ns. The major product ions in the spectrum include photofragment ions (x_4 to x_8 and v_9), the peaks associated with loss of the side chain of amino acids from the precursor ions (m_1, m_3, m_6, and m_8/m_9), and a tryptophan immonium ion (W). Interestingly, the $x_7 + 1$ ion peak appears alone without the corresponding even-electron x_7 ion peak. This radical species seems to have an ion structure to stabilize its radical site. Some y-, Y-, and y*-type ions are also observed with relatively weak intensities. Although some low m/z product ions are missing, high-energy product ions are dominant peaks 300 ns after photoexcitation. The tandem mass spectrum of FSWGAEGQ**K** with a time delay of 1 μs after photodissociation (Figure 7B) is qualitatively similar to that of FSWGAEGQ**R** with a time delay of 13 μs (Figure 6D). In this case, y ion intensities are comparable to those of x-type ions. An increase of the time delay to 5 μs (Figure 7C) results in dominant y-type ion peaks and, significantly, the appearance of some N-terminal fragment ions. In the tandem mass spectrum with a time delay of 13 μs (Figure 7D), the relative intensities of y- to x-type ions become even higher and more N-terminal fragment ions (a_5, a_6, c_7, and c_8) appear.

For a quantitative comparison of thermal and high energy fragment ions, peak intensities of thermal y and y* ions observed were summed and divided by the total intensity of x, x + 1, x + 2 photofragment ions in the same mass spectrum. These ratios at the four time delays are represented as ● and ■ for FSWGAEGQ**R** and FSWGAEGQ**K**, respectively, in Figure 8. For FSWGAEGQ**R**, this ratio linearly increases from 0.19 to 0.67 between 300 ns and 13 μs. Note that the high-energy photofragment ions are still more intense than the thermal fragment ions at 13 μs. For FSWGAEGQ**K**, in contrast, the ratio

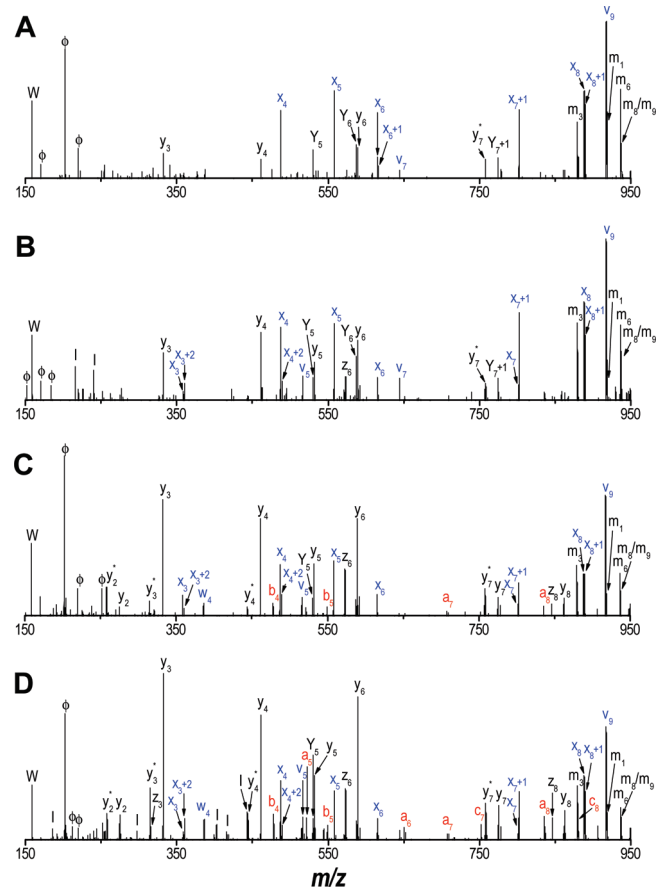

Figure 7. Tandem mass spectra by 157 nm photodissociation of FSWGAEGQ**K** with time delays between photoexcitation and mass analysis of (A) 300 ns, (B) 1 μs, (C) 5 μs, and (D) 13 μs.

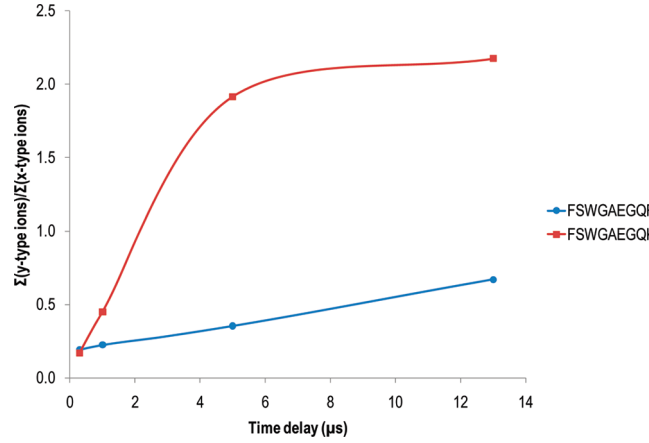

Figure 8. The ratio of peak intensities of y-type ions relative to x-type ions as a function of the time delay (y-type ions include y and y* ions and x-type ions consist of x, x + 1, and x + 2 ions).

sharply increases from 0.17 to 1.9 when the time delay varies from 300 ns to 5 μs and reaches 2.2 with a time delay of 13 μs. This indicates that thermal fragmentation induced by intramolecular vibrational redistribution and proton mobilization begins on a submicrosecond time scale and occurs up to 5 μs after photoexcitation for lysine-containing peptides. Time-resolved analysis of peptide fragmentation has previously been performed using surface-induced dissociation (SID) in a MALDI TOF mass analyzer[69] and UV photodissociation in a MALDI tandem TOF

(68) Harrison, A. G. *Mass Spectrom. Rev.* **1997**, *16*, 201–217.

apparatus.[70] These experiments have focused on submicrosecond to several microsecond fragmentation time frames. However, these studies differ from the current experiments in two respects. First, they utilized SIMION simulation results to extract time information from the spectra, whereas we experimentally control the time parameter. Second, they did not compare the time evolution of arginine- and lysine-containing peptide fragments.

In summary, arginine-containing peptide FSWGAEGQ**R** results in photodissociation tandem mass spectra dominated by high-energy photofragment ions (x- and v-type ions) up to 1 μs after photoexcitation. With a time delay of 13 μs, low-energy fragment ions (y-type ions) become comparable to photodissociation product ions in relative peak intensities. For lysine-containing peptide FSWGAEGQ**K**, in contrast, y-type ions are as abundant as photofragment ions 1 μs after photoexcitation, which is about 10 times faster than FSWGAEGQ**R**. With a time delay of 5 μs or longer, N-terminal fragment ions appear and y-type ions become dominant peaks in the tandem mass spectra. Although some factors other than gas-phase basicity can also influence the observed abundance of product ions in the tandem mass spectra, the study of two peptides having the same sequence except for the C-terminal basic residue should minimize these effects. Thus, the faster onset of thermal fragmentation processes for FSWGAEGQ**K** than FSWGAEGQ**R** can be attributed mainly to the difference in the gas phase basicity of the two C-terminal residues.

CONCLUSIONS

A new type of LIT/o-TOF mass spectrometer has been designed and constructed for the time-dependent observation of product ions by UV photodissociation of peptide ions. Unlike conventional o-TOF instruments, photofragmentation occurs in the TOF source just before orthogonal ion extraction for mass analysis. The collisional damping time before ions exit the back section of the trap and the fall time of the axial extraction pulse on the back lens strongly affect axial ion beam spreading in the TOF source. To detect axially divergent photodissociation product ions, a large detector is positioned below the axis between the trap and the TOF source and the ion reflector is inclined to guide ions toward the detector. A lower axial extraction voltage on the LTQ back lens yields better mass resolution by reducing spatial and kinetic energy distributions of ions on the TOF axis before the orthogonal acceleration pulse. The implementation of a collisional damping system on the transfer octopole slightly increases mass resolution but significantly decreases sensitivity. Photodissociation in the TOF source makes it possible to obtain tandem mass spectra of product ions created less than 1 μs after excitation. Time-dependent observation of product ions from 157 nm photodissociation of NWDAGFGR revealed that high-energy photofragment ions (x- and v-type ions) are major product ions in the mass spectrum up to 1 μs after the laser shot. Thermal fragment ions (y-type ions) become comparable in intensity 5 μs after photoexcitation. Time-dependent 157 nm photodissociation tandem mass spectra of FSWGAEGQ**R** and FSWGAEGQ**K** showed that y-type ions become comparable in intensity to high-energy photofragment ions about 10 times faster in the lysine-containing ion. The instrument can be employed to study the time-dependent evolution of photodissociation of other biomolecules such as oligosacharrides and lipids and to study the effect of laser wavelength on the photofragmentation dynamics.

ACKNOWLEDGMENT

This work was supported by grants from the National Science Foundation (Grants CHE-0431991 and CHE-0518234). We wish to thank the Mechanical and Electrical Instrumentation Services in the Chemistry Department of Indiana University for their excellent craftsmanship in the design and construction of the instrument.

SUPPORTING INFORMATION AVAILABLE

Detailed descriptions of the instrument, the process of axial ion ejection, and supplementary figures as noted in text. This material is available free of charge via the Internet at http://pubs.acs.org.

Received for review June 18, 2009. Accepted September 12, 2009.

AC9013258

(69) Gamage, C. M.; Fernández, F. M.; Kuppannan, K.; Wysocki, V. H. *Anal. Chem.* **2004**, *76*, 5080–5091.

(70) Yoon, S. H.; Kim, M. S. *J. Am. Soc. Mass Spectrom.* **2007**, *18*, 1729–1739.